ACS Catalysis

Research Article

pubs.acs.org/acscatalysis

NMR-Guided Rational Engineering of an Ionic-Liquid-Tolerant Lipase

Erik M. Nordwald,[†] Geoffrey S. Armstrong,[‡] and Joel L. Kaar*,[†]

[†]Department of Chemical and Biological Engineering, [‡]Department of Chemistry and Biochemistry, University of Colorado at Boulder, Boulder, Colorado 80309, United States

ABSTRACT: Biocatalysis in ionic liquids (ILs) is largely limited by the instabilities of enzymes in these solvents, thus negating their auspicious solvent properties. Here, we have engineered an IL-tolerant variant of lipase A (lipA) from *Bacillus subtilis* by examining the site-specific interactions of lipA with 1-butyl-3-methylimidazolium chloride ([BMIM][Cl]). Results of NMR analysis found that [BMIM][Cl] induced structural perturbations near the active site of lipA, underscoring the importance of mediating direct ion interactions with the IL in this region. Mutation of G158 near the active site to glutamic acid resulted in a 2.5-fold improvement in tolerance of lipA to 2.9 M (or 50% v/v) [BMIM][Cl], which correlated with the retention of active site structure. The effect of the G158E mutation was likely the result of inhibition of hydrophobic interactions with the [BMIM] cation. Further analysis of the electrostatic surface of lipA led to the mutation of K44 to glutamic acid to diminish the attraction of chloride anions, which also improved lipA tolerance to [BMIM][Cl]. Beneficial point mutations, which had an additive effect on lipA stability, were combined, resulting in a super stable lipA quadruple mutant (G158E/K44E/R57E/Y49E) with a 7-fold improvement in stability. In comparison, nonspecific charge modification via acetylation and succinylation resulted in only a 1.2- and 1.9-fold improvement in stability, respectively, over wild-type lipA. Ultimately, these results, while providing insight into the nature of the structural effects of ILs on enzymes, highlight the utility of combining NMR and charge engineering to rationally optimize enzyme stability for biocatalysis in ILs.

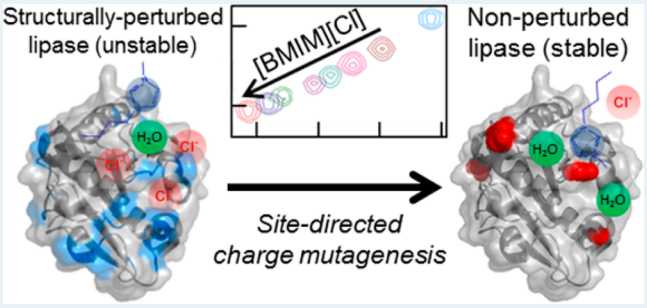

KEYWORDS: *enzyme engineering, ionic liquids, biocatalysis, lipase, heteronuclear single quantum coherence NMR*

1. INTRODUCTION

Despite the immense potential of ionic liquids (ILs) as solvents for biocatalysis for producing pharmaceuticals,[1−3] biofuels,[4−7] and other fine chemicals,[8] rational approaches to improve enzyme tolerance to ILs are inherently needed. Biocatalytic reactions in neat ILs as well as aqueous-IL mixtures are largely limited, because of the denaturation of enzymes by ILs, thus negating the excellent solvent properties of ILs.[9−14] While many approaches to improve the stability of enzymes in ILs have been investigated, conventional approaches, including immobilization, polyethylene glycol modification, and chemical cross-linking, have been, in virtually all cases, unsuccessful in expanding the scope of biocatalysis in IL media.[15−21]

In earlier work, we reported that altering the surface charge of enzymes can markedly enhance the kinetic and thermodynamic stability of enzymes in the presence of the IL 1-butyl-3-methylimidazolium chloride ([BMIM][Cl]).[22,23] Enhancements in kinetic and thermodynamic stability specifically correlated with the ratio of positive-to-negative charged groups on the enzyme surface. In these studies, the impact of changing this ratio was studied by chemically modifying the enzyme surface using nonspecific reactions that randomly target primary amines and carboxylate groups. Lowering this ratio, in particular, led to increased kinetic and thermodynamic stability, which also correlated with exclusion of the chloride (Cl^-) anion from the enzyme surface. Exclusion of the anion from the enzyme surface via electrostatic repulsion may preserve important packing interactions, including hydrogen bonds, which can be disrupted by nucleophilic anions.[24−26]

The stabilization of enzymes against IL-induced denaturation via charge modification presents considerable opportunities for improving the efficiency of biocatalytic reactions in IL environments. As evidence of such opportunities, we have shown that a range of enzymes, including chymotrypsin, lipase, papain, and cellulase can be stabilized from inactivation in aqueous-IL solutions via altering surface charge.[22,23,27] In the case of cellulase, the enzyme preparation (*Trichoderma reesei*) that was modified consisted of a mixture of cellulolytic enzymes, which, upon modification, also showed improved resistance toward lignin inhibition.[27] However, such enhancements in stability by charge modification may be significantly improved with a more detailed understanding of the specific sites in enzymes that are structurally perturbed by ILs. An understanding of the propensity of the constituent cation and anion to perturb specific sites may be used to inform or guide the mutation of these sites to site-specifically mediate changes in solvent environment. Importantly, by site-specifically mediating cation and anion-induced changes in enzyme

Received: July 9, 2014
Revised: September 5, 2014
Published: October 7, 2014

   dx.doi.org/10.1021/cs500978x | ACS Catal. 2014, 4, 4057−4064

structure, functionally important residues and motifs may be more effectively shielded from the denaturing effects of ILs than via nonspecific modifications. Moreover, through site-specific charge engineering, deleterious modifications as well as even neutral modifications, which have a negligible effect on enzyme stability, may also be prevented. The ability to probe direct ion interactions involving ILs with specific sites on protein surfaces was recently demonstrated by Figueiredo and co-workers[28] using NMR spectroscopy.

Herein, we have uniquely combined NMR spectroscopy with charge engineering to rationally engineer the industrially important enzyme lipase A (lipA) from *Bacillus subtilis* for improved tolerance to [BMIM][Cl]. In this approach, two-dimensional heteronuclear single quantum coherence (15N/1H HSQC) NMR was employed to identify residues on the surface of lipA that experience a change in local chemical environment in the presence of [BMIM][Cl]. Analysis of chemical shift perturbations due to changes in solvent environment was used to mutate specific residues to charged amino acids to locally inhibit direct ion interactions with the cation and anion. Furthermore, analysis of the electrostatic map of lipA was used to discern additional residues as candidates for mutation that are potential sites around which chloride may cluster due to strong Coulombic interactions. Upon screening mutants with single point mutations by measuring enzyme half-life ($T_{1/2}$), beneficial mutations were combined to optimize lipA stability and relate lipA stability to sequence and structure. Notably, lipA, like other lipases, catalyzes industrial biotransformations that entail the hydrolysis, formation, and rearrangement of ester bonds in aqueous and nonaqueous media.[29−31] Despite previous attempts to improve enzyme tolerance to ILs via directed evolution,[32−34] this work represents, to the best of our knowledge, the first attempt to rationally engineer an enzyme for improved biocatalysis in IL environments.

2. EXPERIMENTAL SECTION

2.1. Materials. Genomic DNA from *B. subtilis* containing the lipA gene was kindly donated by Robert Batey (University of Colorado, Boulder). The QuikChange lightning mutagenesis kit for site-directed mutation of lipA was purchased from Agilent (Santa Clara, CA). All other chemicals, including [BMIM][Cl] (>98%), 4-nitrophenyl butyrate (pNPB), and N_{15} labeled ammonium chloride (98 at. %) were purchased from Sigma−Aldrich (St. Louis, MO) and used as supplied.

2.2. Enzyme Expression, Purification, and Mutagenesis. To produce recombinant lipA, the gene for lipA (without the pelB leader sequence) was initially PCR amplified from genomic *B. subtilis* DNA and cloned into pET21b, using NdeI and SacI restriction sites. The forward and reverse primers used for amplification were 5′-GATATACATATG-GCTGAACACAATCCAGTCGTTATG-3′ and 5′-GATATTGAGCTCTCATTAATTCGTATTCTGGCCCCC-3′, respectively. Upon cloning, the pET21b lipA vector was transformed to BL21 (DE3) *Escherichia coli*, which was grown in growth media (Luria broth) at 37 °C and 200 rpm with 100 mg/L ampicillin. Expression of lipA was induced via the addition of 1 mM isopropyl β-D-1-thiogalactopyranoside also at 37 °C. After 1.5 days, soluble lipA that was secreted during expression was collected and dialyzed against 50 mM MES buffer (pH 6.8) prior to use in stability assays without further purification.

For 15N/1H HSQC experiments, lipA was expressed in M9 minimal media with N_{15} ammonium chloride as the sole nitrogen source and purified from insoluble cell lysate. Following an induction period of 2.5 days, cells were harvested via centrifugation and lysed using a PandaPlus 2000 homogenizer (GEA, Inc., Columbia, MD). To purify lipA, the insoluble portion of the lysate was dissolved in 6 M GnHCl, which was subsequently diluted 20-fold with 10 mM sodium phosphate (pH 5.5) to promote refolding of the enzyme. The refolded enzyme was separated via centrifugation at 15 000 g for 15 min and finally purified by cation exchange chromatography. The resulting purified enzyme was dialyzed against 10 mM sodium phosphate buffer (pH 7.0) concentrated to 8 mg/mL, and was estimated quantitatively to be >98% pure by SDS-PAGE.

For site-directed mutagenesis, lipA was mutated by using the QuikChange lightning mutagenesis kit. The correct insertion of all mutations was verified by sequencing.

2.3. LipA Stability Assay. Stability to IL-induced inactivation was assayed by incubating wild-type or mutant lipA (0.01 mg/mL) in 20 mM MES buffer with 2.9 M or (50% v/v) [BMIM][Cl] (final pH 6.5) at 35 °C with constant shaking (100 rpm). Inactivation of lipA was followed by periodically removing aliquots (735 μL) and assaying residual lipA activity by measuring the enzymatic hydrolysis of pNPB (3 mM), which was prepared in acetonitrile (2% v/v final concentration). The initial rate of pNPB hydrolysis was assayed spectrophotometrically by continuously monitoring the release of 4-nitrophenyl at 412 nm at room temperature. To determine $T_{1/2}$, the resulting stability curves were fit to a first-order, reversible (N⇔U) unfolding model.

2.4. NMR Experiments. 15N/1H HSQC spectra of wild-type and G158E lipA (400 μM) were recorded at 298 K for 30 min using a 900 MHz DD2 spectrometer with a cryogenic probe (Agilent Technologies). For sample preparation, 0−0.29 M (or 5% v/v) [BMIM][Cl] was added to the enzyme in 10 mM sodium phosphate (final pH 7.0) with 5% v/v D_2O. Peak assignments, which were previously reported by Augustyniak and co-workers,[35] were transferred from the Biological Magnetic Resonance Bank (entry 18574). Of the 171 residues for which peak assignments were reported, 165 of the residues in the spectra of lipA were easily assignable based on overlapping peak resonances. The remaining six peaks could not be assigned with confidence due to weak signal-to-noise or because of uncertainty in the peak position. For determination of chemical shift perturbations (Δ chemical shift), the combined ΔH_1 and ΔN_{15} perturbation was calculated using the following equation:

$$\Delta \text{ chemical shift} = ((\Delta H_1)^2 + (\alpha \Delta N_{15})^2)^{0.5}$$

In the above equation, ΔH_1 and ΔN_{15} are the H_1 and N_{15} chemical shift perturbations (in ppm), respectively, and α is a scaling factor for which a value of 0.17 was used.[36,37] In the analysis of Δ chemical shift, a minimum cutoff of 0.05 ppm was used as the threshold for significance.

3. RESULTS AND DISCUSSION

3.1. 15N/1H HSQC Analysis of IL-Induced Chemical Shift Perturbations in LipA. With the goal of rationally enhancing IL tolerance of lipA, specific residues that are structurally perturbed by the addition of [BMIM][Cl] due to local changes in solvent environment were initially determined

dx.doi.org/10.1021/cs500978x | ACS Catal. 2014, 4, 4057−4064

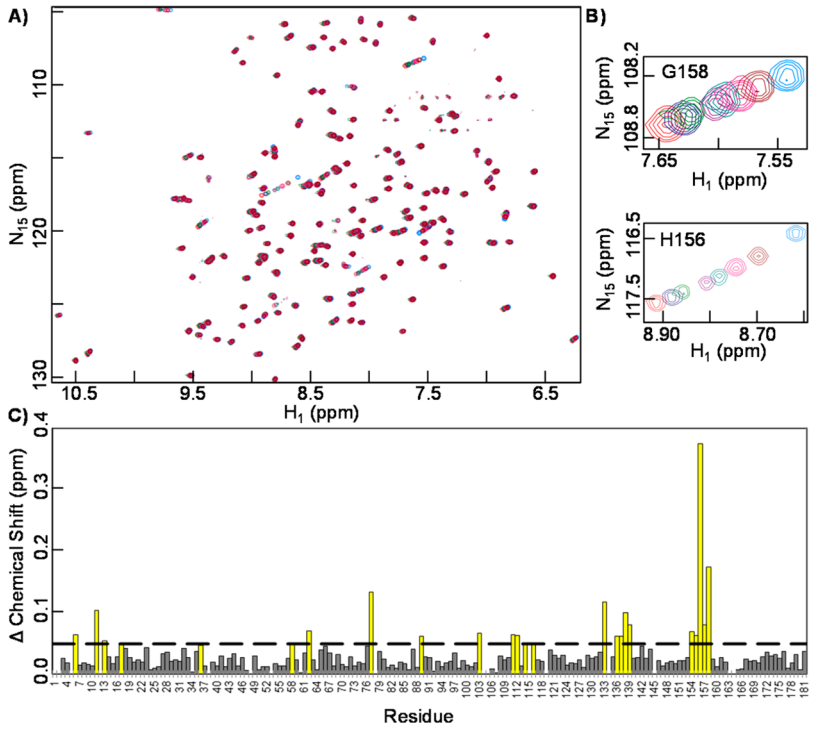

Figure 1. 15N/1H HSQC spectra of wild-type lipA in the presence of [BMIM][Cl]. (A) Overlay of spectra with 0 (light blue), 0.029 (brown), 0.057 (pink), 0.086 (cyan), 0.11 (purple), 0.17 (green), 0.23 (navy), and 0.29 (red) M [BMIM][Cl]. (B) Enlarged views of spectral changes to residues G158 and H156, which experienced the largest chemical shift perturbations in lipA upon titration with [BMIM][Cl]. (C) Chemical shift perturbations with 0.29 M (or 5 vol %) [BMIM][Cl] for all residues in lipA. The dashed line at 0.05 ppm represents the threshold used for significance of chemical shift perturbations. All residues with significant chemical shift perturbations are represented by yellow bars. For unassigned residues, bars representing chemical shift perturbations were omitted.

by 15N/1H HSQC NMR. Local changes in enzyme and, more broadly, protein structure can be probed using 15N/1H HSQC NMR via analysis of perturbations in the peak resonances of individual residues within the enzyme. In analogous studies, Figueiredo and co-workers[28] previously used 15N/1H HSQC NMR to examine IL-induced structural changes in a model four-bundle helix protein by [BMIM][Cl] along with other ILs, demonstrating the applicability of this technique for our purpose. Notably, their results identified a number of charged as well as nonpolar residues that experienced significant chemical shift perturbations, implicating electrostatic as well as hydrophobic ion interactions. Hydrophobic ion interactions may specifically arise from interactions involving the alkyl side chain of the [BMIM] cation with nonpolar residues and regions on the protein surface. In addition, 15N/1H HSQC NMR has been also used to examine the effects of organic solvents on enzyme and protein structure, including for a thermostabile lipase mutant also from *B. subtilis*.[38−40]

Results of 15N/1H HSQC analysis of lipA with [BMIM][Cl] found multiple peak perturbations involving surface residues that are likely involved in direct ion interactions with the IL. The perturbation of select residues are readily apparent in Figure 1A, which shows an overlay of 15N/1H HSQC spectra for lipA with 0−0.29 M (or 5% v/v) [BMIM][Cl]. Of important note, at the concentrations of IL used, the global structure of the enzyme was retained, resulting in shifts of only residues thought to be perturbed as a result of direct ion interactions. Residues that experienced the largest shifts include the catalytic residue H156 and G158 (see Figure 1B for an enlarged view of the spectral shifts of H156 and G158), which are part of a patch of residues involving V154, G155, and I157 that were also perturbed. The magnitude of the perturbations of the residues in this patch is shown in Figure 1C, which shows the chemical shift perturbations for all residues in lipA with 0.29 M [BMIM][Cl]. Because of the nonpolar nature of many of the residues in this patch, these residues are presumably perturbed by the cation through hydrophobic interactions with the butyl chain of [BMIM]. To confirm that these residues were perturbed by ion interactions and not changes in pH, which alter the ionization state of H156, control spectra were collected at pH 6.9 (at the largest IL concentration, the addition of [BMIM][Cl] reduced the solution pH 0.05 units from pH 7). In the control spectra, residues V154−G158 did not appear to shift, verifying the role of direct ion interactions between lipA and the IL in perturbing this patch on the enzyme surface (data not shown). In addition, around the active site region, G11, G13, and residues V136−Y139, as well as the other residues of the catalytic triad S77 and D133, were also perturbed. Notably, residues V136−139 are situated close to the positively charged residues R107 and R142, which may attract the chloride anion to this region.

While it is interesting to consider perturbations near the active site, which may directly contribute to the loss of enzyme activity, shifts in other regions of lipA may similarly be important for IL tolerance. A patch of surface residues that are distant from the active site that encompasses N89, G111, K112, L114, and G116 also experienced significant chemical shifts (Figure 1C). Shifts in this patch may be attributed to chloride interactions due to the presence of neighboring positively charged residues (K88, R107, and K122) as hypothesized to occur near the active site. Several other nonpolar residues in different locations throughout the enzyme were also perturbed,

dx.doi.org/10.1021/cs500978x | *ACS Catal.* 2014, 4, 4057−4064

including V6, F17, F58, V62, and G103. Interestingly, of the total 23 residues that were perturbed in lipA by [BMIM][Cl], the majority of these residues (13) are located in flexible loop regions, as opposed to structured β-sheets (1) or α-helices (9). Because of the inherent flexibility of these residues, these residues may be more susceptible to structural perturbations at low IL concentrations. To better understand the location, exposure, secondary structure, and proximity of the residues that are perturbed, the structurally perturbed residues were mapped onto the crystal structure of lipA (see Figure 2).

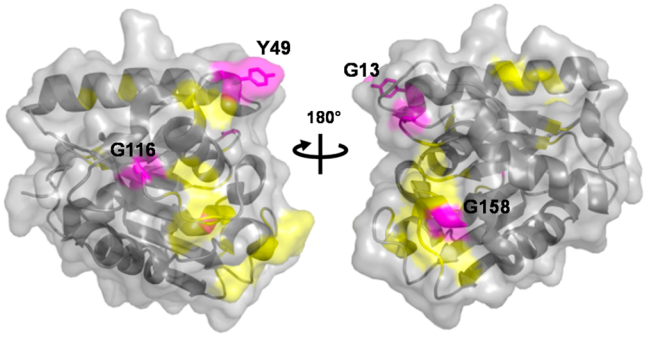

Figure 2. Structure of lipA (Protein DataBank code: 1ISP) with a map of chemical shift perturbations due to direct ion interactions with [BMIM][Cl]. Residues that experienced significant chemical shift perturbations (≥0.05 ppm) with the addition of 0.29 M (5 v/v %) IL are colored yellow. The residues in magenta with side chains showing represent sites that were mutated to glutamic acid to inhibit direct ion interactions with the IL by site-directed mutagenesis.

3.2. Impact of Site-Directed Mutagenesis on IL Tolerance of LipA. Based on proximity to structurally perturbed sites, residues on the surface of lipA were subsequently considered for site-directed mutagenesis. The goal of mutagenesis in this case was to inhibit direct ion interactions with the cation and anion by altering the local electrostatic environment through mutating candidate residues to glutamic acid. We hypothesized that substitution of glutamic acid would, as we have shown previously,[22] lead to exclusion of the Cl^- ion through repulsive Coulombic interactions. Furthermore, we predicted that glutamic acid mutations would weaken hydrophobic interactions with the butyl chain of [BMIM] by disrupting the hydrophobicity of nonpolar regions on the surface of lipA. In principle, the mutation of surface residues to aspartic acid would exert a similar effect, although perhaps to a lesser degree, because of the further protrusion of glutamic acid into the solvent environment. The residues that were mutated were G13, Y49, G116, and G158, which were themselves structurally perturbed (G13, G116, G158) or in close proximity to structurally perturbed sites (Y49) in lipA (see Figure 2). Although not significantly perturbed itself, residue Y49 is nearby the perturbed residue N89, which was not directly mutated, because of potential steric clashes with neighboring residues (namely, Y85). In addition to their proximity to perturbed sites, the mutated residues are highly solvent exposed and non-hydrogen bonding in the crystal structure of lipA.

To determine the effect of G13E, Y49E, G116E, and G158E substitutions on lipA tolerance to [BMIM][Cl], individual variants with each point mutation were prepared by site-directed mutagenesis. Tolerance of wild-type and mutant lipA to [BMIM][Cl] was measured by assaying residual enzyme activity over time upon incubation in buffer containing 2.9 M (50% v/v) [BMIM][Cl]. With the exception of G116E, all of the mutations resulted in a significant increase in the $T_{1/2}$ of lipA, relative to wild-type lipA, thereby improving the tolerance of lipA to [BMIM][Cl] (see Figure 3). The most significant

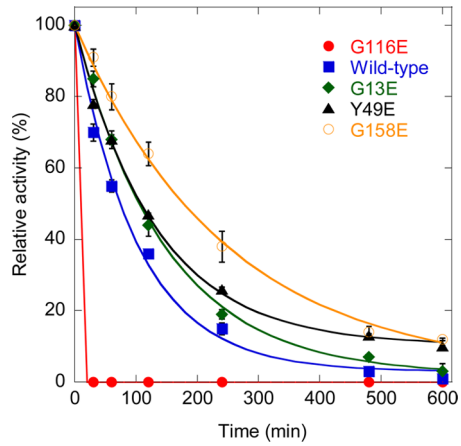

Figure 3. Activity retention profiles for wild-type (solid blue square, ■), G116E (solid red circle, ●), G13E (solid green diamond, ◆), Y49E (solid black triangle, ▲), and G158E (open orange circle, ○) lipA in 20 mM MES buffer and 2.9 M (50 v/v %) [BMIM][Cl] (pH 6.5) at 35 °C.

increase in $T_{1/2}$ was observed for the G158E mutant ($T_{1/2}$ = 183 min), which extended the $T_{1/2}$ of lipA, relative to wild-type ($T_{1/2}$ = 74 min), by nearly 2.5-fold. Substitution of glutamic acid at this position presumably alters the polarity around V154−G158, reducing the propensity of [BMIM] interactions in this region and, furthermore, preventing structural perturbations to the catalytic H156, D133, and S77. Given the large impact of the G158 mutation on $T_{1/2}$, the results of stability studies suggest that the interactions with [BMIM] in this region may be particularly denaturing and thus critical to lipA stability. For the Y49E ($T_{1/2}$ = 108 min) and G13E ($T_{1/2}$ = 105 min) mutations, improvements in $T_{1/2}$ of lipA of ∼1.5-fold were observed for each. Because of the proximity of G13 to the active site, the mutation of this residue to glutamic acid likely also leads to the retention of active site structure while preventing cation and anion interactions. In the case of the G116E mutation, substitution of G116 to glutamic acid resulted in destabilization of lipA, perhaps by disrupting local hydrogen bonding and nearby salt bridges.

Because the glutamic acid mutations alter enzyme charge, an alternative explanation for the observed improvements in stability of lipA G13E, Y49E, and G158E variants is that the added negative charge prevents IL-induced salting out of the enzyme. Specifically, it is plausible that the charge mutations lead to increased solubility of lipA in the presence of [BMIM][Cl], which, in turn, leads to an increase in $T_{1/2}$. To confirm that the stabilization of lipA upon mutation was due to the inhibition of IL-induced unfolding rather than salting out, lipA solubility in the presence of [BMIM][Cl] was directly measured. For measuring salting out, the concentration of soluble lipA in the presence of [BMIM][Cl] was monitored over time by monitoring absorbance of lipA at 280 nm. The concentration of [BMIM][Cl] used for salting out assays was the equivalent to that used in the above stability studies. Notably, at this concentration of IL, the absorbance of wild-

dx.doi.org/10.1021/cs500978x | ACS Catal. 2014, 4, 4057−4064

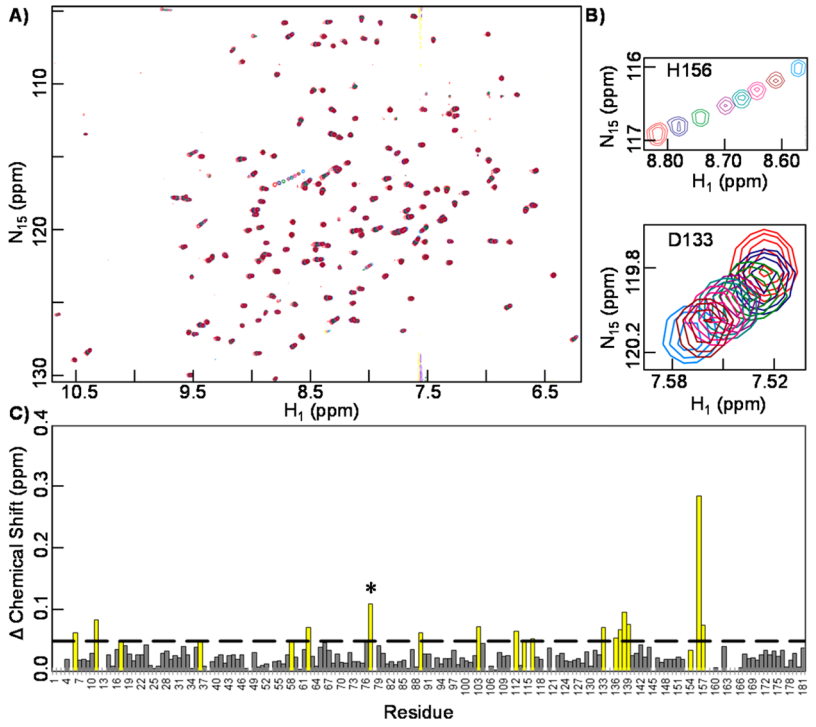

Figure 4. 15N/1H HSQC spectra of G158E lipA in the presence of [BMIM][Cl]. (A) Overlay of spectra with 0 (light blue), 0.029 (brown), 0.057 (pink), 0.086 (cyan), 0.11 (purple), 0.17 (green), 0.23 (navy), and 0.29 (red) M [BMIM][Cl]. (B) Enlarged views of spectral changes to residues H156 and D133 upon titration with [BMIM][Cl]. (C) Chemical shift perturbations with 0.29 M (or 5 v/v %) [BMIM][Cl] for all residues in lipA. The dashed line at 0.05 ppm represents the threshold used for significance of chemical shift perturbations. Yellow bars represent residues that experienced a significant chemical shift perturbation in wild-type lipA. For unassigned residues, bars representing chemical shift perturbations were omitted. The asterisk (*) denotes that, because of weak signal at 0.29 M [BMIM][Cl], the chemical shift perturbation for S77 was determined using the 0.23 M [BMIM][Cl] sample.

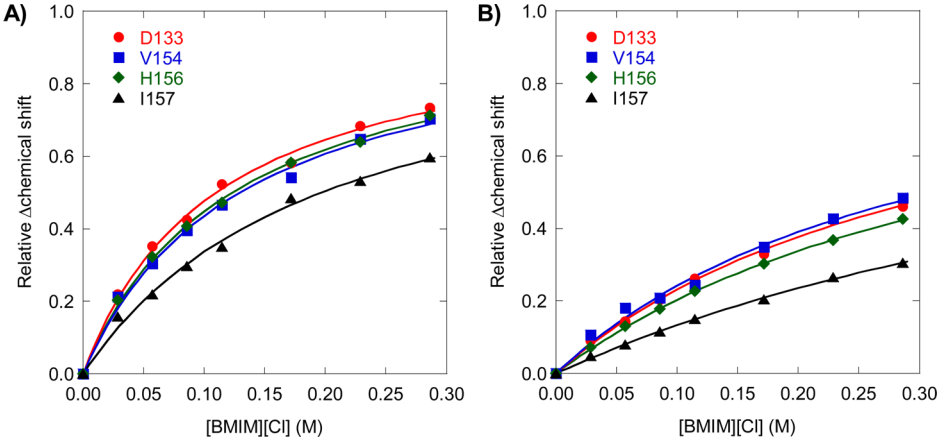

Figure 5. Dependence of chemical shift perturbations on [BMIM][Cl] concentration for residues D133 (solid red circle, ●), V154 (solid blue square, ■), H156 (solid green diamond, ◆), and I157 (solid black triangle, ▲) in (A) wild-type lipA and (B) G158E lipA. All of the residues analyzed are within 10 Å of amino acid 158 and experienced a Δ chemical shift of ≥0.05 ppm in wild-type lipA with the addition of 0.29 M (5% v/v) [BMIM][Cl]. Curves were fit to a Langmuir isotherm model to determine the theoretical maximum shift at each site for normalization of the perturbations at each IL concentration.

type lipA decreased by a negligible amount (<5%) over 1 week, indicating minimal if any precipitation of lipA occurred. Given the lack of precipitation of wild-type lipA over this period, it is highly unlikely that salting out, although not measured for lipA variants, was the cause of lipA inactivation in stability studies. In addition, inhibition studies of lipA activity as a function of varying [BMIM][Cl] concentration showed little difference between the variants and wild-type lipA. Based on this, the mutations appear to affect only the kinetic stability of the enzyme and, conversely, do not alter the specific activity of lipA in the presence of [BMIM][Cl].

3.3. Effect of G158E on Structural Perturbations in the Active Site of LipA. Of the glutamic acid mutations that stabilize lipA, the G158E mutation is of particular interest, because of the magnitude of its stabilizing effect and proximity to the active site. The structural basis for the stabilization of lipA upon mutation of G158 to glutamic acid was elucidated by 15N/1H HSQC analysis of G158E lipA with [BMIM][Cl].

dx.doi.org/10.1021/cs500978x | ACS Catal. 2014, 4, 4057−4064

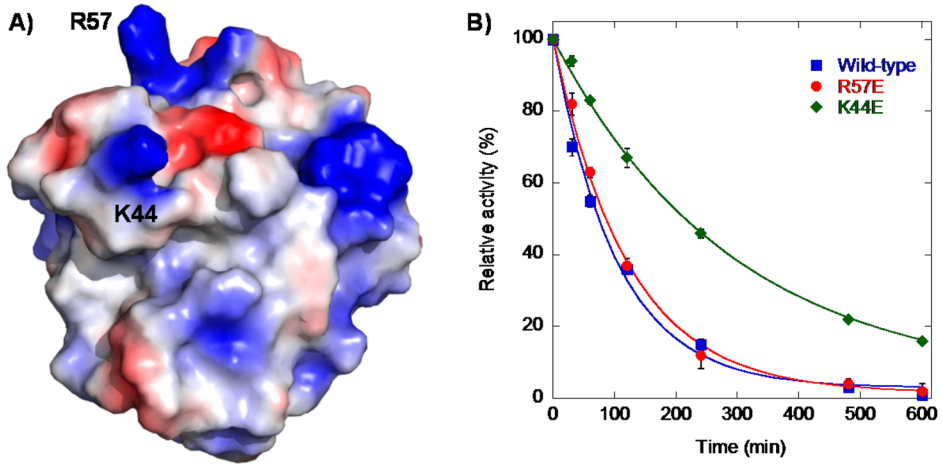

Figure 6. Effect of glutamic acid mutations based on analysis of surface electrostatics. (A) Electrostatic map of the surface of lipA, indicating the positions of the positive-charged K44 and R57, which are highly exposed. (B) Activity retention profiles for wild-type (blue square, ■), R57E (solid red circle, ●), and K44E (solid green diamond, ◆) lipA in 20 mM MES buffer and 2.9 M (50 vol %) [BMIM][Cl] (pH 6.5) at 35 °C.

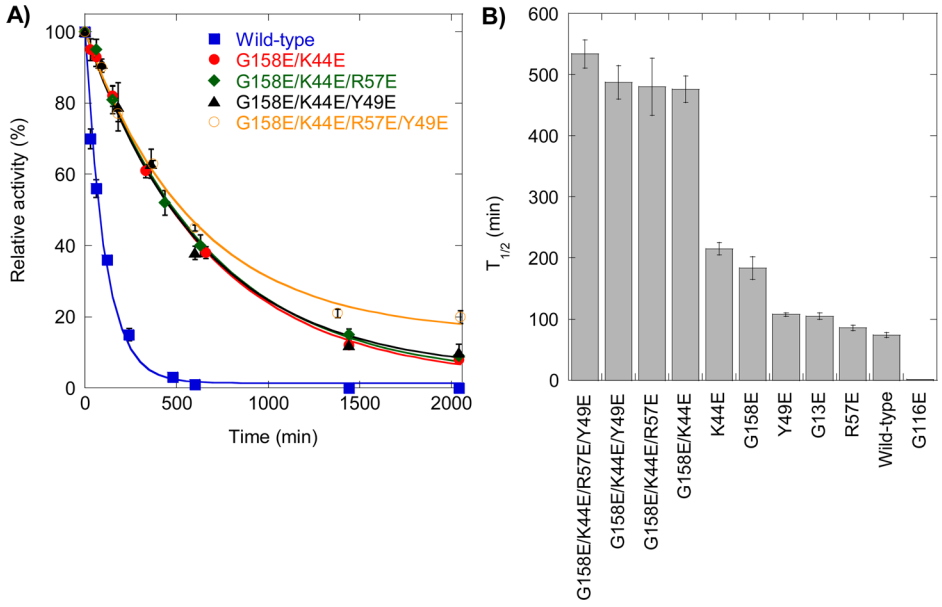

Figure 7. Optimization of lipA tolerance to [BMIM][Cl] by combining beneficial glutamic acid mutations. (A) Activity retention profiles for wild-type (blue square, ■), G158E/K44E (solid red circle, ●), G158E/K44E/R57E (solid green diamond, ◆), G158E/K44E/Y49E (solid black triangle, ▲), and G158E/K44E/R57E/Y49E (open orange circle, ○) lipA in 20 mM MES buffer and 2.9 M (50 vol %) [BMIM][Cl] (pH 6.5) at 35 °C. (B) The $T_{1/2}$ values for wild-type and all lipA variants based on activity retention profiles, assuming reversible, first-order unfolding.

Peak assignments for G158E lipA were inferred based on the juxtaposition of resonances, relative to that in the spectra of wild-type lipA. Although the spectra of the G158E lipA was not assigned directly, the majority of the resonance peaks in G158E could be identified, including the specific area around the active site (155 of 171 residues were assigned for G158E lipA). As for wild-type lipA, the resonance peaks in the spectra of G158E lipA were distinct and well-dispersed, which facilitated the identification of peak resonances. Importantly, all of the residues in G158E lipA that are perturbed shifted in the same direction as in the spectra of wild-type lipA with [BMIM][Cl]. While many of the residues around the mutation site could be assigned, changes in the chemical shift upon mutation prevented the assignment of E158 in the spectra of the mutant lipA.

Analysis of the active site region of lipA in the 15N/1H HSQC spectra of G158E lipA with 0−0.29 M (or 5 vol %) [BMIM][Cl], similar to that observed with wild-type lipA, showed obvious perturbations (Figure 4A). However, the magnitude of the chemical shift perturbations for residues in the active site region overall were significantly weaker than that for wild-type lipA with equivalent [BMIM][Cl] concentrations. In particular, perturbations in H156 were markedly smaller in the mutant lipA (Figure 4B and C). In addition to the magnitude of the shifts being weaker, the dependence of the observed shifts on IL concentration in G158E lipA was diminished relative to those in wild-type lipA. The dependence of chemical shifts for all residues within 10 Å of residue 158 that were structurally perturbed by [BMIM][Cl] was determined for wild-type lipA (Figure 5A) and G158E lipA (Figure 5B). Accordingly, structural perturbations in the active

dx.doi.org/10.1021/cs500978x | ACS Catal. 2014, 4, 4057−4064

site region of G158E lipA were less sensitive to IL concentration than in the active site region of wild-type lipA. To analyze the sensitivity of chemical shifts on IL concentration, the shifts were normalized to the theoretical maximum shift at each site by fitting the shifts to a Langmuir isotherm model as described previously.[28] Because E158 could not be assigned in the 15N/1H HSQC spectra, analysis of chemical shift perturbations of the mutated residue was omitted from the structural characterization of G158E lipA. Ultimately, the 15N/1H HSQC results provide evidence that the G158E mutation stabilizes lipA from inactivation by [BMIM][Cl] via increasing the retention of active site structure.

3.4. Analysis of Electrostatic Surface of LipA. The electrostatic map of the surface of lipA was analyzed to complement the use of NMR to identify surface exposed residues in lipA involved in direct ion interactions. Analysis of the electrostatic map of lipA specifically revealed two residues that point outward from the enzyme surface, which are highly positively charged. These residues, K44 and R57, although not in the active site, may attract Cl^- anions to the enzyme surface, resulting in destabilization of the tertiary structure of lipA (Figure 6A). Interestingly, K44 is located in a flexible loop that is adjacent to G11 and G13, which were structurally perturbed by [BMIM][Cl] in 15N/1H HSQC analysis. Therefore, it is plausible that the perturbation of G11 and G13 is the indirect result of the attraction of Cl^- anions to this region of the enzyme by K44. The role of K44 in direct ion interactions with chloride was confirmed by mutation of K44 to glutamic acid, which resulted in a 2.9-fold improvement in the $T_{1/2}$ of lipA in IL tolerance assays (Figure 6B). Mutation of R57, which is nearby the perturbed residues F58 and V62, had only a minimal, although still beneficial (1.2-fold improvement in $T_{1/2}$), impact on lipA stability in the presence of [BMIM][Cl].

3.5. Combinatorial Optimization of LipA IL Tolerance. Individual single point mutations that had beneficial effects on lipA tolerance to [BMIM][Cl] were combined to optimize lipA stability for biocatalysis in IL environments. By combining mutations, a super stable lipA quadruple mutant (G158E/K44E/R57E/Y49E) was created, which was over 7 times more tolerant to [BMIM][Cl] than wild-type lipA (Figure 7A and 7B). Notably, the super stable G158E/K44E/R57E/Y49E quadruple mutant retained ~20% activity after nearly 1.5 days and appeared to reach an equilibrium state. In all cases, the effect of combining beneficial mutations on lipA tolerance to [BMIM][Cl] was additive, suggesting that effect of each mutation is individual from one another. The additive nature of the mutations is perhaps not surprising, given that the mutations that were combined are distant from one another in lipA and thus presumably would not interact. In optimizing the IL tolerance of lipA, the G13E and K44E mutations were not combined, because of the proximity of G13 and K44 in the folded state of lipA. It was presumed that the simultaneous mutation of both residues would result in repulsion between the neighboring glutamic acids, which would have a deleterious effect on lipA stability. Although the combined mutations improved the stability of lipA in the presence of [BMIM][Cl], the apparent melting temperatures of the quadruple mutant and wild-type lipA in the absence of IL were almost identical (~53 °C), suggesting that the impact of the mutations on stability was specific to ILs.

To underscore the improvement in stability afforded by this site-specific approach, lipA was also modified by acetylation and succinylation as a means of nonspecific charge engineering. Having previously been shown to mediate direct anion interactions involving ILs in our earlier work,[22] acetylation and succinylation provide a simple route to replace the positive charge of amines with neutral and acid groups, respectively. In comparison to the super stable G158E/K44E/R57E/Y49E quadruple mutant, acetylation and succinylation resulted in only a 1.2- and 1.9-fold improvement in $T_{1/2}$, respectively, over wild-type lipA. This drastic difference in stabilizing effects upon site-specific versus random charge engineering highlight the importance of mediating ion interactions with functionally important residues.

4. CONCLUSIONS

We have engineered an ionic liquid (IL)-tolerant lipA through site-directed mutagenesis of surface residues to charged amino acids, which mediate direct ion interactions with the solvent. Mutation of surface residues to glutamic acid in structurally perturbed regions of lipA, including near the active site, improved lipA tolerance to [BMIM][Cl] by as much as 2.5-fold. Substitution of glutamic acid was found to have a large effect on lipA stability upon mutation of, in particular, G158, which is located within a hydrophobic region near the active site of lipA. This effect, which correlated with the retention of active site structure in structural studies, was likely the result of the inhibition of hydrophobic interactions with the [BMIM] cation. Tolerance of lipA to [BMIM][Cl] was also significantly enhanced via similar mutation of positively charged surface residues (i.e., K44) that may attract Cl^- ions to glutamic acid. When combined, the effects of beneficial mutations were additive, resulting in a super stable lipA quadruple mutant (G158E/K44E/R57E/Y49E), which had a 7-fold improvement in stability relative to wild-type lipA. These results ultimately shed light on the effect of direct ion interactions on enzyme stability in ILs and the impact of mediating these interactions site-specifically via charge engineering. The combination of NMR and charge engineering to site-specifically visualize and mediate direct ion interactions represents a powerful approach to improve enzyme stability to ILs.

AUTHOR INFORMATION

Corresponding Author

*Address: Department of Chemical and Biological Engineering, University of Colorado at Boulder, Campus Box 596, Boulder, CO 80309. Tel.: (303) 492-6031. Fax: (303) 492-4341. E-mail: joel.kaar@colorado.edu.

Notes

The authors declare no competing financial interest.

ACKNOWLEDGMENTS

We are grateful for support for this work from an EAGER grant from the National Science Foundation (No. CBET 1347737). We are also thankful to Deborah Wuttke, for helpful discussion on the collection and analysis of NMR data, and to Sean Yu McLoughlin and Lauren Woodruff, for their assistance with cloning and expression of LipA.

REFERENCES

(1) Galonde, N.; Nott, K.; Debuigne, A.; Deleu, M.; Jerome, C.; Paquot, M.; Wathelet, J. P. *J. Chem. Technol. Biotechnol.* **2012**, *87*, 451−471.

(2) Kaftzik, N.; Wasserscheid, P.; Kragl, U. *Org. Process Res. Dev* **2002**, *6*, 553−557.

(3) Tee, K. L.; Roccatano, D.; Stolte, S.; Arning, J.; Bernd, J.; Schwaneberg, U. *Green Chem.* **2008**, *10*, 117−123.
(4) Zhang, K. P.; Lai, J. Q.; Huang, Z. L.; Yang, Z. *Bioresour. Technol.* **2011**, *102*, 2767−2772.
(5) Ha, S. H.; Lan, M. N.; Lee, S. H.; Hwang, S. M.; Koo, Y. M. *Enzyme Microb. Technol.* **2007**, *41*, 480−483.
(6) Bose, S.; Barnes, C. A.; Petrich, J. W. *Biotechnol. Bioeng.* **2012**, *109*, 434−443.
(7) Li, C. L.; Knierim, B.; Manisseri, C.; Arora, R.; Scheller, H. V.; Auer, M.; Vogel, K. P.; Simmons, B. A.; Singh, S. *Bioresour. Technol.* **2010**, *101*, 4900−4906.
(8) Park, S.; Kazlauskas, R. J. *Curr. Opin. Biotechnol.* **2003**, *14*, 432−437.
(9) Kaar, J. L.; Jesionowski, A. M.; Berberich, J. A.; Moulton, R.; Russell, A. J. *J. Am. Chem. Soc.* **2003**, *125*, 4125−4131.
(10) van Rantwijk, F.; Sheldon, R. A. *Chem. Rev.* **2007**, *107*, 2757−2785.
(11) Baker, G. A.; Heller, W. T. *Chem. Eng. J.* **2009**, *147*, 6−12.
(12) Constantinescu, D.; Weingartner, H.; Herrmann, C. *Angew. Chem., Int. Ed.* **2007**, *46*, 8887−8889.
(13) Baker, S. N.; Zhao, H.; Pandey, S.; Heller, W. T.; Bright, F. V.; Baker, G. A. *Phys. Chem. Chem. Phys.* **2011**, *13*, 3642−3644.
(14) Heller, W. T.; O'Neill, H. M.; Zhang, Q.; Baker, G. A. *J. Phys. Chem. B* **2010**, *114*, 13866−13871.
(15) Nakashima, K.; Maruyama, T.; Kamiya, N.; Goto, M. *Chem. Commun.* **2005**, *34*, 4297−4299.
(16) Persson, M.; Bornscheuer, U. T. *J. Mol. Catal. B: Enzym.* **2003**, *22*, 21−27.
(17) Schofer, S. H.; Kaftzik, N.; Wasserscheid, P.; Kragl, U. *Chem. Commun.* **2001**, *5*, 425−426.
(18) Toral, A. R.; de los Rios, A. P.; Hernandez, F. J.; Janssen, M. H. A.; Schoevaart, R.; van Rantwijk, F.; Sheldon, R. A. *Enzyme Microb. Technol.* **2007**, *40*, 1095−1099.
(19) Vafiadi, C.; Topakas, E.; Nahmias, V. R.; Faulds, C. B.; Christakopoulos, P. *J. Biotechnol.* **2009**, *139*, 124−129.
(20) van Rantwijk, F.; Secundo, F.; Sheldon, R. A. *Green Chem.* **2006**, *8*, 282−286.
(21) Zhao, H.; Jones, C. L.; Cowins, J. V. *Green Chem.* **2009**, *11*, 1128−1138.
(22) Nordwald, E. M.; Kaar, J. L. *J. Phys. Chem. B* **2013**, *117*, 8977−8986.
(23) Nordwald, E. M.; Kaar, J. L. *Biotechnol. Bioeng.* **2013**, *110*, 2352−2360.
(24) Klahn, M.; Lim, G. S.; Seduraman, A.; Wu, P. *Phys. Chem. Chem. Phys.* **2011**, *13*, 1649−1662.
(25) Jaeger, V. W.; Pfaendtner, J. *ACS Chem. Biol.* **2013**, *8*, 1179−1186.
(26) Burney, P. R.; Pfaendtner, J. *J. Phys. Chem. B* **2013**, *117*, 2662−2670.
(27) Nordwald, E. M.; Brunecky, R.; Himmel, M. E.; Beckham, G. T.; Kaar, J. L. *Biotechnol. Bioeng.* **2014**, *111*, 1541−1549.
(28) Figueiredo, A. M.; Sardinha, J.; Moore, G. R.; Cabrita, E. J. *Phys. Chem. Chem. Phys.* **2013**, *15*, 19632−19643.
(29) Adlercreutz, P. *Chem. Soc. Rev.* **2013**, *42*, 6406−6436.
(30) Nagarajan, S. *Appl. Biochem. Biotechnol.* **2012**, *168*, 1163−1196.
(31) Stergiou, P. Y.; Foukis, A.; Filippou, M.; Koukouritaki, M.; Parapouli, M.; Theodorou, L. G.; Hatziloukas, E.; Afendra, A.; Pandey, A.; Papamichael, E. M. *Biotechnol Adv.* **2013**, *31*, 1846−1859.
(32) Liu, H. F.; Zhu, L. L.; Bocola, M.; Chen, N.; Spiess, A. C.; Schwaneberg, U. *Green Chem.* **2013**, *15*, 1348−1355.
(33) Lehmann, C.; Bocola, M.; Streit, W. R.; Martinez, R.; Schwaneberg, U. *Appl. Microbiol. Biotechnol.* **2014**, *98*, 5775−5785.
(34) Chen, Z. W.; Pereira, J. H.; Liu, H. B.; Tran, H. M.; Hsu, N. S. Y.; Dibble, D.; Singh, S.; Adams, P. D.; Sapra, R.; Hadi, M. Z.; Simmons, B. A.; Sale, K. L. *PLoS One* **2013**, *8*, e79725.
(35) Augustyniak, W.; Wienk, H.; Boelens, R.; Reetz, M. T. *Biomol. NMR Assignments* **2013**, *7*, 249−252.
(36) Farmer, B. T. *Nat. Struct. Biol.* **1996**, *3*, 995−997.
(37) Williamson, M. P. *Prog. Nucl. Magn. Reson. Spectrosc.* **2013**, *73*, 1−16.
(38) Byerly, D. W.; McElroy, C. A.; Foster, M. P. *Protein Sci.* **2002**, *11*, 1850−1853.
(39) Kamal, M. Z.; Yedavalli, P.; Deshmukh, M. V.; Rao, N. M. *Protein Sci.* **2013**, *22*, 904−915.
(40) McLachlan, G. D.; Slocik, J.; Mantz, R.; Kaplan, D.; Cahill, S.; Girvin, M.; Greenbaum, S. *Protein Sci.* **2009**, *18*, 206−216.